Published in final edited form as:
J Neural Eng. 2013 October ; 10(5): 056005. doi:10.1088/1741-2560/10/5/056005.

Long term, stable brain machine interface performance using local field potentials and multiunit spikes

Robert D. Flint[1], **Zachary A. Wright**[1], **Michael R. Scheid**[1], and **Marc W Slutzky**[1,2,3,4]

Robert D. Flint: r-flint@northwestern.edu; Zachary A. Wright: zachary-wright@northwestern.edu; Michael R. Scheid: mr.scheid@u.northwestern.edu; Marc W Slutzky: mslutzky@northwestern.edu

[1]Department of Neurology, Northwestern University, Chicago IL 60611

[2]Department of Physiology, Northwestern University, Chicago IL 60611

[3]Department of Physical Medicine & Rehabilitation, Northwestern University, Chicago IL 60611

[4]Rehabilitation Institute of Chicago, Chicago, IL 60611

Abstract

Objective—Brain machine interfaces (BMIs) have the potential to restore movement to people with paralysis. However, a clinically-viable BMI must enable consistently accurate control over time spans ranging from years to decades, which has not yet been demonstrated. Most BMIs that use single-unit spikes as inputs will experience degraded performance over time without frequent decoder re-training. Two other signals, local field potentials (LFPs) and multi-unit spikes (MSPs), may offer greater reliability over long periods and better performance stability than single-unit spikes. Here, we demonstrate that LFPs can be used in a biomimetic BMI to control a computer cursor.

Approach—We implanted two rhesus macaques with intracortical microelectrodes in primary motor cortex. We recorded LFP and MSP signals from the monkeys while they performed a continuous reaching task, moving a cursor to randomly-placed targets on a computer screen. We then used the LFP and MSP signals to construct biomimetic decoders for control of the cursor.

Main results—Both monkeys achieved high-performance, continuous control that remained stable or improved over nearly 12 months using an LFP decoder that was not retrained or adapted. In parallel, the monkeys used MSPs to control a BMI without retraining or adaptation and had similar or better performance, and that predominantly remained stable over more than six months. In contrast to their stable online control, both LFP and MSP signals showed substantial variability when used offline to predict hand movements.

Significance—Our results suggest that the monkeys were able to stabilize the relationship between neural activity and cursor movement during online BMI control, despite variability in the relationship between neural activity and hand movements.

Corresponding author: Marc W. Slutzky, MD, PhD, 303 E. Superior Ave., Lurie 8-121, Chicago, IL 60611, mslutzky@northwestern.edu.

The authors have no conflicts of interest to disclose.

Introduction

The ability to decode movement intent from the cerebral cortex has spurred accelerating development of brain machine interfaces (BMIs) in the last decade. BMIs provide a way to control an external device directly [1–4] or restore limb movement [5–7] using cortical signals. Biomimetic BMIs are trained using normal movement, providing an intuitive mapping between body movements and the external effector [8]. Most biomimetic BMIs have used single-unit action potentials, or spikes, but it is difficult to retain the same single units for more than a few weeks with multielectrode arrays [9]. Worse, these implants suffer neuron dropout on a majority of electrodes after a few years [10]. Multi-unit spikes (MSPs), defined here as threshold-crossing events, may have greater longevity and stability than single-unit spikes [11], while providing similar decoding accuracy [12]. Local field potentials (LFPs) also provide highly accurate offline reconstructions of reach kinematics [13–18], grasp kinematics [19], and muscle activity [20]. Furthermore, LFP-based movement decoding remains accurate in the absence of spiking activity at the same electrode [18, 21], suggesting that LFPs may exhibit better longevity than single units.

The relationship between single-unit spike activity in motor cortex and reach kinematics has been shown to be stable over several hours to a few days [22, 23], although others have shown substantial variability in this relationship over the same timescale [24, 25]. The relationship between carefully-selected single-unit spikes and BMI-controlled cursor movement has also been shown to be stable over a few weeks [26], but not over longer periods. Since MSPs, and in particular LFPs, represent aggregate neuronal activity sampled from a wider spatial extent than single units [27–29], it has been hypothesized that these signals may be less sensitive to nonstationarity in individual neurons' activity and thus may enable more stable BMI performance [30].

The current study demonstrates, for the first time, continuous real-time control of a computer cursor using LFPs in a biomimetic BMI. Two monkeys used a static LFP decoder to achieve stable, accurate cursor control over 350 days. We also demonstrate that monkeys could use an MSP-based BMI to achieve stable performance for nearly 200 days.

Materials and Methods

All procedures were performed under protocols approved by the Northwestern University Institutional Animal Care and Use Committee.

Random target pursuit task – hand control

Two adult rhesus macaques, one male and one female (monkeys C and M) used a two-link manipulandum to move a cursor (1-cm diameter circle) within a rectangular planar workspace (20 cm × 20 cm) in a random-target pursuit task (Figure 1). The task consisted of moving the cursor to a series of targets placed at random locations on the screen, and holding within each target for 0.1 s. The monkeys were required to correctly hit 6 consecutive targets before receiving a reward. Target size was 2 cm × 2 cm square. Trials in which the monkey required more than 2 s to reach a target, or exited a target before the hold period elapsed, were labelled failures.

Microelectrode array implantation

In each monkey, we surgically implanted a 96-channel silicon electrode array (Blackrock Microsystems) into the primary motor cortex (M1) contralateral to the arm used to control the cursor. Electrode shank length was 1.5 mm. During surgery, monkeys were anesthetized with isoflurane (2–3 %). Electrode arrays were implanted in the arm/hand area, as determined by referencing cortical landmarks and by intraoperative electrical stimulation with a silver ball electrode (2–5 mA, 200 μs pulses at 60 Hz). During stimulation, a reduced level of isoflurane (< 0.5 MAC) was supplemented with intravenous remifentanil (0.15 – 0.30 μg/kg/min) to reduce suppression of cortical excitability. Anaesthetic depth was assessed at all times by monitoring jaw muscle tone and vital signs. The arrays were grounded to the Cereport pedestal and referenced to a platinum wire with 3 mm exposed wire length placed under the dura. Both monkeys were given postoperative analgesics buprenorphine and meloxicam for 2 and 4 days, respectively. Further details of the surgery can be found in [31].

Data acquisition and decoder training

All neural and behavioural data were recorded using a 96-channel Multiple Acquisition Processor (Plexon, Inc, Dallas, Tx). We calculated the end-point position of the hand from the manipulandum's joint angles (sampled at 1 kHz) and downsampled to 20 Hz for analysis. LFP signals were band-pass filtered from 0.7 Hz to 300 Hz (or 0.7 Hz to 170 Hz on 32 of the channels) and sampled at 1 kHz. To build the static online control decoder for each monkey, we used ten minutes of continuously-recorded reaching activity. For each LFP channel, we calculated the local motor potential (LMP; [32, 33] as a sliding 256 ms window of the LFP signal to provide a sample every 50 ms. In addition to the LMP, we computed the spectral power of each LFP channel by applying a 256-point Hanning window (overlapped by 206 points) and calculating the squared amplitude of the windowed signal's discrete Fourier transform. We averaged spectral power within the following frequency bands: 0–4 Hz, 7–20 Hz, 70–115 Hz, 130–200 Hz, and 200–300 Hz. As the total feature set of 576 features (for 96 recorded signals) could lead to overfitting, we performed dimensionality reduction as in prior studies. We computed the absolute value of the correlation coefficient ($|R|$) between each feature and the velocity in each dimension, and selected the 150 features with highest mean $|R|$ as inputs to a Wiener cascade decoder [34–36]. We previously used the Wiener cascade filter with offline LFP decoding of movement [18] and EMG [20]. The Wiener cascade included 10 lags, for a total filter length of 0.5 s.

Multiunit spikes were preprocessed by high-pass filtering at 300 Hz and sampled at 40 kHz. The threshold on each channel was set by visual inspection once at the beginning of the first MSP session and kept constant for the duration of this study. The mean thresholds over all channels were 3.8 and 4.9 standard deviations above baseline for monkeys C and M, respectively. MSP firing rates in 50-ms bins were used as the inputs to a Wiener cascade filter (including 10 causal lags).

Brain control using LFPs and MSPs

Monkeys performed online control (brain control) in the random target pursuit task by moving the cursor to a randomly-located, 4×4-cm square target with a 0.1 s hold time,

within 10 s of target appearance, for a liquid reward. The monkeys were free to move their arms during brain control. Cursor position was determined as the integral of predicted cursor velocity, updated every 50 ms. Velocity predictions were made in real time using custom software running on a Linux platform. For LFP-based brain control, we extracted features every 50 ms. The same LFP features selected to build the decoder were used to predict x- and y-velocities. For MSP control, binned spike times were used in the BMI to predict velocity. Both forms of brain control used an offset to adjust the velocity predictions at each 50-ms time step. We reasoned that in the random target pursuit task, the mean velocity in each direction should approach zero over a sufficiently long time span. Therefore, we applied a high-pass filter (time constant 60 s) to the predicted velocities before integrating to obtain cursor position.

During the course of the study, a few LFP channels became corrupted with high-amplitude, low-frequency noise. In some cases, the cause was a broken wire in a cable or connector, and in others it may have been a problem on the array itself. We removed bad channels from the static decoder by setting all entries associated with that channel to zero in the decoder's transformation matrix. Once a channel was removed in this manner, it was not restored, and the static decoder was not recalculated. Low-frequency noise did not occur on MSP channels, so they were not removed. A few MSP units did not produce threshold crossings on some days, but we did not observe a channel that became permanently devoid of spikes.

Monkeys used two distinct LFP-based decoders, built on days 0 and 231 for monkey M and days 0 and 224 for monkey C (see Figure 2). Each decoder was trained on 10 minutes of hand control data and then held fixed through all testing days.

Performance measures

To quantify performance during brain control, we measured the overall success rate, defined as the ratio of rewarded trials to total number of trials in an epoch. Multiple brain control epochs, usually lasting 20–40 minutes, were recorded in each day's session, and monkeys performed 3–5 epochs per week of brain control. In addition to success rate, we calculated three kinematic variables from successful trials: (1) normalized time-to-target, (2) normalized path length, and (3) the index of performance, according to Fitts' law. The first two kinematic measures were calculated as in Suminski et al. [37]. The normalized path length essentially quantifies path curvature; a value of 1.0 corresponds to a perfectly straight line. This measure is related to the movement variability index developed by Mackenzie et al [38] and was used previously to quantify BMI performance in a paralyzed human subject [39]. The index of performance was similar to the throughput quantity specified in part 9 of the ISO 9241 standard for non-keyboard computer input devices. It was calculated according to the Shannon formulation of Fitts' law [40, 41]:

$$IP = \frac{ID}{TT}$$

where TT was the time to target, and ID was the index of difficulty

$$ID = \log_2 \left(\frac{D}{W} + 1 \right).$$

Here, D was the distance between the start and the end of a reach, and W was the width of a target. The median across trials for each epoch was reported.

Chance performance

We computed a chance performance level for success rate during brain control by applying the LFP decoder to phase-randomized LFPs from brain control epochs [17, 18]. We used the cursor trajectories predicted by this method, and the actual sequence of target locations, to calculate success rate in the same manner as described above, with a 10 s time limit to reach each target. We performed this analysis on 10 minutes of data from each of 3 different days. We repeated the procedure of randomization, prediction, and evaluation 1000 times on each day's data.

Stability of offline decoding

We tested the hypothesis that using a static decoder to make offline predictions of hand control files would result in decreased performance over time. For each monkey, we selected 9 hand control epochs from which to build LFP decoders, and 9 epochs from which to build MSP decoders. In each case, one of the decoders was the one used for online brain control. We split the initial (day 0) hand control epoch into 10-minute segments and trained a decoder using data from the first segment. We then held that decoder static, and tested it on (1) the second segment from day 0, and (2) subsequent hand control epochs, up to 100 days later. We measured decoding accuracy by computing the coefficient of determination (R^2) between predicted and actual hand velocities. We selected hand control testing data from epochs spaced throughout the length of the study on a subset of the days brain control was performed.

Results

Monkeys M and C performed the continuous random pursuit task under brain control using two LFP decoders (LFP1, LFP2), and one multiunit spike decoder (MSP). A typical day's experiment included a hand control epoch (10–20 minutes of task execution), as well as an LFP control epoch (20–30 minutes) and/or an MSP control epoch (20–30 minutes.). Table 1 shows the frequency with which the monkeys used each decoder. From day 16 to day 98, the monkeys' weekly exposure to the LFP1 BMI was limited to 1–2 epochs/week, due to their participation in an unrelated study. Following that period, the monkeys performed the random-target BMI task 5 days/week. Each day's experiment lasted 1–2 hours. In the course of a typical week, we varied the order of decoders used within the brain control epochs. By the end of the study, we had removed 12 channels each from monkey C and M's LFP1 decoders due to noise (see Methods). Only 2 and 1 channels were removed from monkey C and M's LFP2 decoders, respectively, during the course of brain control with those decoders. Monkey C averaged 84 ± 2 (mean ± SD) MSP units, while Monkey M had a remarkably stable 84 ± 0.3 MSP units.

Accurate BMI performance with static LFP and MSP decoders

Both monkeys demonstrated high performance during brain control (Table 2). This was true for both LFP-based and MSP-based brain control. In each case, the performance was well above chance success rate. (Chance performance was 5 ± 3% and 4 ± 3% for monkeys C and M, respectively.) Indeed, performance with both types of decoders was similar to that seen in other spike-based brain control studies (see Discussion). When averaged over all epochs, spike-based brain control outperformed LFP-based brain control in most measures ($p<10^{-6}$ for all measures comparing LFP1 vs. MSP or LFP2 vs. MSP using t-tests), except for success rate (p=0.63, LFP1 vs. MSP) and cursor speed (p=0.20, LFP2 vs. MSP) in monkey C. However, this difference declined over time (Figure 2), and the trends suggest that the two performances will eventually converge.

To quantify the performance trends, we calculated Pearson's correlation coefficient between the performance measure and recording day (Table 3). Both monkeys improved their success rate over time when using the LFP1 decoder. Success rate using the MSP decoder was stable in monkey C but declined in monkey M. Time to target (Figure 2B) improved or remained stable for both LFP and MSP decoders. The index of performance improved or remained stable over time, except for MSP in monkey C (Figure 2C). The success rate and index of performance for spikes were more variable than for LFPs. Path lengths remained stable for monkey C, but lengthened slightly for monkey M (Figure 2D). Monkey M's more curved paths did not result in a lower success rate or time to target, however (Figure 2A and 2B, right), indicating a successful strategy of compensation was employed, i.e., increasing the mean cursor speed (Figure 2E, right). Cursor speed increased for both LFP decoders, while it remained stable for the MSP decoders (Figure 2E). Thus, the overall trends were stable to improving performance for LFPs, and stable to declining performance for spikes.

To quantify further the effects of time on performance, we divided the brain control epochs for each decoder into two groups, early (epochs from the first half of the study) and late (epochs from the second half of the study). The monkeys' overall success rate and time to target measures both improved significantly from early to late epochs using the LFP1 decoder (t-test, Bonferroni-corrected for multiple comparisons, see Figure 3), while path length remained constant for monkey C and increased slightly for monkey M. Spike control results were mixed. For monkey C, all measured performance variables remained stable (Figure 3B–D, left panels), but monkey M's success rate and path lengths both worsened significantly (Figure 3A, D, right panels). Thus, LFP control results generally improved or remained stable, while spike control results remained stable in one monkey and declined slightly in the other.

Offline decoding of hand movements with static decoders shows variable performance

The stable-to-improving performance we observed when the monkeys used either LFPs or MSPs for online control could be attributable to stable input signals, adaptation by the monkeys, or both. Therefore, we measured the stability of hand velocity decoding performance offline, using a static decoder. This approach prevents the influence of closed-loop effects on performance. We found significantly reduced accuracy in decoding for almost all epochs after day 0 compared to the accuracy on day 0 (Figure 4). Across 9

decoders, monkeys C and M had average R^2 of 0.24 ± 0.01 (69% decrease from day 0) and 0.3 ± 0.01 (57% decrease) after day 0, respectively, for LFPs (mean ± SE, Figure 4 left panels). Their performance after day 0 for MSPs was 0.39 ± 0.01 (40% decrease) and 0.6 ± 0.01 (20% decrease), respectively (Figure 4 right panels). The mean across decoders changed little over time after day 0 (Figure 4 B, C). However, performance of individual decoders was highly variable for both LFPs and MSPs (Figure 4A).

Stability of input signals

As a first approximation of signal stability, we calculated the mean value of each LFP feature (log band power or LMP amplitude) or MSP unit firing rate over the length of each brain control epoch, and normalized to the maximum value for each feature (or firing rate). We performed this computation for features or units included in the LFP1 and MSP static decoders. The LFP features exhibited a remarkable stability over the length of the study (shown for monkey M in Figure 5A). A few aberrations in this pattern (e.g., vertical lines at session 91) were due to a loose connector that was not discovered until the end of the session. MSP firing rates were much more variable from day to day (Figure 5B), with the exception of a few units visible near the top of the figure. Monkey C exhibited respectively similar levels of stability for LFPs and MSPs.

Discussion

This study is the first to use a biomimetic, LFP-based BMI to achieve continuous, online control of a computer cursor. Both LFP- and MSP-based BMIs provided high levels of overall performance, although those using MSPs in general performed slightly better. However, the performance trends suggest that LFP and MSP performance may ultimately converge to similar values over time using a fixed decoder. Moreover, both LFPs and MSPs showed extremely long-lasting, stable performance in closed-loop BMI control. Using static decoders, the LFP-based BMIs performed stably for nearly a year, and the MSP-based BMIs only slightly less so for nearly 200 days.

Biomimetic BMI using LFPs

Several studies have shown that the accuracy of movement decoded offline from intracortical LFPs approaches that using spikes [14, 17–20, 32]. However, until now there have been no published reports of biomimetic BMIs that used LFPs to control continuous cursor movement. Two studies have demonstrated control of a binary state BMI using LFPs [42, 43]. Other groups have used a biofeedback approach to control a BMI with subdural (ECoG) or epidural signals [44–49]. Biofeedback approaches map brain signals to cursor movement in a more abstract fashion, such as mapping movement of different hands to different cursor directions. In contrast, biomimetic BMIs establish a more direct mapping between the brain signals' normal function and behavioural outputs. Therefore, biomimetic BMIs likely impose a lower cognitive burden on the user. This hypothesis is supported by the observation that the monkeys in this study, similar to those in a prior study using biomimetic BMIs [26], switched among multiple BMI decoders each day with little difficulty or transition time.

Overall, the performance of the LFP- and MSP-based BMIs compare favourably with reports in the literature, such as a spike-driven BMI using daily-retrained decoders in a random pursuit task (78% success rate, 0.33 s/cm time to target, and path length of 3.7 averaged over two monkeys, [37]). This performance was also similar to that of two human subjects using daily-retrained decoders ([39], 0.29 s/cm mean performance) and to that of two monkeys using a static decoder in a center-out task ([26], mean 0.54 s/cm). The index of performance reported here also compares favourably with previously reported values with an EEG-based BMI ([47], 0.55 bits/s), a spike-based BMI in paralyzed humans (~0.43 bits/s, Figure 2C from [10]), and a MSP-based BMI in monkeys (0.67 bits/s, [50]). We present these comparisons for context, but note that there are substantial differences among the studies that make such comparisons inexact, including decoder type, behavioural task and prior training, electrode type and location, species, and presence of brain injury [10, 39]. Finally, our BMIs used, on average, 84 MSPs and 125 LFP features, compared to 15 [26], 44 [37], or 80 units [39] in prior studies.

Stability of performance and neural signals

We hypothesized that an LFP-based BMI would provide stable performance, without decoder recalibration, over long time periods. We also hypothesized that MSP-based BMI performance would be less stable over time. The evidence presented here shows that LFP-based BMIs allowed stable-to-improving performance for about one year. While MSP success rate (but not other measures) declined slowly in one monkey, it was stable in the other monkey for about 6 months. One prior study showed stable performance for 5 days using a biofeedback-type ECoG-based BMI [51]. Ganguly and Carmena [26] showed stable BMI control using a static decoder for up to 19 days, including only carefully-selected single-unit spikes that showed highly stable waveform characteristics. A preliminary report also showed stable control for several weeks using an adapted decoder of MSPs which was later held static [52]. Thus, our results show that LFPs and MSPs are capable of sustaining stable performance far longer than previously demonstrated.

In monkey M, MSP success rate declined slightly over time. The reason for this decline is not certain; however, it only occurred in one monkey and other performance metrics did not decline significantly for this decoder. It is possible that the lower MSP success rate at the end of the study was still acceptably high to this monkey. Alternatively, factors such as array movement or degradation could have affected the success rate. LFP control performance did not decline in this animal. LFPs are derived from a larger number of neurons than are MSPs, and thus the effects on LFPs due to changes in a few neurons are likely negligible. Thus, it is possible that electrode issues could affect MSPs more than LFPs.

In contrast to the low initial performance and steep learning curve seen in [26], our monkeys had high initial performance using both LFP and MSP-based BMIs and either stable or gradually improving performance over a few months (Figure 2A). This difference may be related to the larger signal source population used here, which likely supplied richer information about movement. Also, our monkeys' arms were not restrained, while those in [26] were required not to move. Either of these factors may have contributed to the different

pattern seen here, which was also seen in prior spike BMI studies with greater numbers of neurons [37].

The ensemble neural representation of arm movements is highly stable over 1–2 days [24]. The evidence for signal stability is less clear at the single neuron level, with some finding variability [24, 25] and others finding great stability [22, 23] over 1–2 days. Our results suggest that the picture is somewhat different over much longer timescales, and/or during brain control instead of hand movement. Individual MSPs showed highly variable firing rates over weeks to months, while LFPs were much more stable (Figure 5). In addition, ensemble representation of arm movements (offline decoding performance, Figure 4) using individual static decoders fluctuated substantially from day to day. When averaged over all decoders, there was a significant performance decline after day 0, followed by relatively stable performance. This "steady-state" offline decoding performance using either MSPs or LFPs is comparable to results from prior offline studies using spikes ([24]; R^2~0.42) and ECoG with static decoders ([53]; R^2~0.5). Online performance, however, remained stable or improved, despite the fluctuating, degraded performance in offline decoding over time. This implies that, during brain control, either the monkeys were able to learn a stable representation of the BMI decoder or they were able to compensate for daily fluctuations. The former would suggest that visual feedback during brain control plays a role in ensuring stable neural representations of movement. Overall, these results suggest that a more detailed analysis of signal stability over long timescales is warranted.

Implications for clinical neuroprostheses

Our results demonstrate that a BMI can be controlled online with high accuracy and stable–to-improving performance over many months with a static, biomimetic decoder using either LFPs or MSPs. The ability to use a static BMI decoder would eliminate the need to recalibrate the decoder on a frequent basis. It could also enable BMI users to improve their performance over time, as our monkeys did with the LFP1 decoder. It also appears likely that inclusion of both spikes and LFPs would yield superior performance, compared to using either source signal alone [14, 54]. Intracortical implants typically lose discriminable units on half or more of their electrodes within a few years [10], but LFP signals can decode movement even on electrodes in which spikes are absent [18], suggesting that they may provide greater longevity. Thus, using LFPs may enable BMI devices with stable performance and longer lifetimes.

The monkeys in this study were unrestrained during brain control, but their movements differed greatly from the movements during hand control and were not consistent from epoch to epoch. Obviously paralyzed patients can only attempt to move, but attempting to move produces brain activity that is more similar to movement—more biomimetic—than to imagined movement, or other strategies monkeys use when they perform brain control without moving. As a control experiment, we did restrain both arms in a few sessions (data not shown); initial performance was poorer and improved more slowly. BMI control can be learned by paralyzed subjects [3, 39, 55–57], but typically required longer learning periods than seen here or in [26] to achieve high performance.

This study was not designed to optimize BMI control. We used relatively simple methods of feature selection that likely could be improved. Further, the electrode arrays were placed at depths optimized for spike recording (layer V of the cortex), whereas LFPs have been shown to be more informative at shallower depths such as layer II/III [58]. Thus, it seems likely we could improve LFP-based BMI performance simply by recording at shallower depths. It is also possible that decoder adaptation could improve BMI performance [50, 59, 60]. For example, Gilja et al. improved the throughput performance of their decoder from approximately 0.67 bits/s to approximately 1.6 bits/s using an adaptive retraining algorithm [50]. Our results suggest that brain control using MSPs and LFPs is similar enough that methods shown to improve MSP decoding may also improve LFP decoding. However, the gradual improvement displayed by our monkeys in online control reinforces the idea that the natural ability of the motor cortex to adapt its own patterns of activity is likely the most powerful adaptive mechanism that any BMI can exploit. Thus, any changes to the decoder should be designed to avoid undermining learning [61].

Acknowledgments

This study was funded by NIH grant 5K08 NS060223. We would like to thank Matt Baumann, Eric Lindberg, and Nicholas Sachs for their contributions to the implementation of the BMI, and Lee Miller for helpful comments on the manuscript and use of equipment.

References

1. Serruya MD, Hatsopoulos NG, Paninski L, Fellows MR, Donoghue JP. Instant neural control of a movement signal. Nature. 2002; 416:141–2. [PubMed: 11894084]
2. Carmena JM, Lebedev MA, Crist RE, O'doherty JE, Santucci DM, Dimitrov DF, Patil PG, Henriquez CS, Nicolelis MA. Learning to control a brain-machine interface for reaching and grasping by primates. PLoS Biol. 2003; 1:1–16.
3. Hochberg LR, Serruya MD, Friehs GM, Mukand JA, Saleh M, Caplan AH, Branner A, Chen D, Penn RD, Donoghue JP. Neuronal ensemble control of prosthetic devices by a human with tetraplegia. Nature. 2006; 442:164–71. [PubMed: 16838014]
4. Velliste M, Perel S, Spalding MC, Whitford AS, Schwartz AB. Cortical control of a prosthetic arm for self-feeding. Nature. 2008; 453:1098–101. [PubMed: 18509337]
5. Moritz CT, Perlmutter SI, Fetz EE. Direct control of paralysed muscles by cortical neurons. Nature. 2008; 456:639–42. [PubMed: 18923392]
6. Pohlmeyer EA, Oby ER, Perreault EJ, Solla SA, Kilgore KL, Kirsch RF, Miller LE. Toward the restoration of hand use to a paralyzed monkey: Brain-controlled functional electrical stimulation of forearm muscles. PLoS One. 2009; 4:e5924. [PubMed: 19526055]
7. Ethier C, Oby ER, Bauman MJ, Miller LE. Restoration of grasp following paralysis through brain-controlled stimulation of muscles. Nature. 2012; 485:368–71. [PubMed: 22522928]
8. Jackson A, Fetz EE. Interfacing with the computational brain. IEEE Trans Neural Syst Rehabil Eng. 2011; 19:534–41. [PubMed: 21659037]
9. Dickey AS, Suminski A, Amit Y, Hatsopoulos NG. Single-unit stability using chronically implanted multielectrode arrays. J Neurophysiol. 2009; 102:1331–9. [PubMed: 19535480]
10. Simeral JD, Kim SP, Black MJ, Donoghue JP, Hochberg LR. Neural control of cursor trajectory and click by a human with tetraplegia. 1000 days after implant of an intracortical microelectrode array. J Neural Eng. 2011; 8:025027. [PubMed: 21436513]
11. Chestek CA, Gilja V, Nuyujukian P, Foster JD, Fan JM, Kaufman MT, Churchland MM, Rivera-Alvidrez Z, Cunningham JP, Ryu SI, Shenoy KV. Long-term stability of neural prosthetic control signals from silicon cortical arrays in rhesus macaque motor cortex. J Neural Eng. 2011; 8:045005. [PubMed: 21775782]

12. Fraser GW, Chase SM, Whitford A, Schwartz AB. Control of a brain-computer interface without spike sorting. Journal of neural engineering. 2009; 6:055004. [PubMed: 19721186]
13. Pesaran B, Pezaris JS, Sahani M, Mitra PP, Andersen RA. Temporal structure in neuronal activity during working memory in macaque parietal cortex. Nat Neurosci. 2002; 5:805–11. [PubMed: 12134152]
14. Mehring C, Rickert J, Vaadia E, Cardosa De Oliveira S, Aertsen A, Rotter S. Inference of hand movements from local field potentials in monkey motor cortex. Nat Neurosci. 2003; 6:1253–4. [PubMed: 14634657]
15. Rickert J, Oliveira SC, Vaadia E, Aertsen A, Rotter S, Mehring C. Encoding of movement direction in different frequency ranges of motor cortical local field potentials. J Neurosci. 2005; 25:8815–24. [PubMed: 16192371]
16. Stark E, Abeles M. Predicting movement from multiunit activity. J Neurosci. 2007; 27:8387–94. [PubMed: 17670985]
17. Bansal AK, Vargas-Irwin CE, Truccolo W, Donoghue JP. Relationships among low-frequency local field potentials, spiking activity, and three-dimensional reach and grasp kinematics in primary motor and ventral premotor cortices. J Neurophysiol. 2011; 105:1603–19. [PubMed: 21273313]
18. Flint RD, Lindberg EW, Jordan LR, Miller LE, Slutzky MW. Accurate decoding of reaching movements from field potentials in the absence of spikes. J Neural Eng. 2012; 9:046006. [PubMed: 22733013]
19. Zhuang J, Truccolo W, Vargas-Irwin C, Donoghue JP. Decoding 3-d reach and grasp kinematics from high-frequency local field potentials in primate primary motor cortex. IEEE Trans Biomed Eng. 2010; 57:1774–84. [PubMed: 20403782]
20. Flint RD, Ethier C, Oby ER, Miller LE, Slutzky MW. Local field potentials allow accurate decoding of muscle activity. J Neurophysiol. 2012; 108:18–24. [PubMed: 22496527]
21. Bokil HS, Pesaran B, Andersen RA, Mitra PP. A method for detection and classification of events in neural activity. IEEE Trans Biomed Eng. 2006; 53:1678–87. [PubMed: 16916103]
22. Chestek CA, Batista AP, Santhanam G, Yu BM, Afshar A, Cunningham JP, Gilja V, Ryu SI, Churchland MM, Shenoy KV. Single-neuron stability during repeated reaching in macaque premotor cortex. J Neurosci. 2007; 27:10742–50. [PubMed: 17913908]
23. Stevenson IH, Cherian A, London BM, Sachs NA, Lindberg E, Reimer J, Slutzky MW, Hatsopoulos NG, Miller LE, Kording KP. Statistical assessment of the stability of neural movement representations. J Neurophysiol. 2011; 106:764–74. [PubMed: 21613593]
24. Carmena JM, Lebedev MA, Henriquez CS, Nicolelis MA. Stable ensemble performance with single-neuron variability during reaching movements in primates. J Neurosci. 2005; 25:10712–6. [PubMed: 16291944]
25. Rokni U, Richardson AG, Bizzi E, Seung HS. Motor learning with unstable neural representations. Neuron. 2007; 54:653–66. [PubMed: 17521576]
26. Ganguly K, Carmena JM. Emergence of a stable cortical map for neuroprosthetic control. PLoS Biol. 2009; 7:e1000153. [PubMed: 19621062]
27. Katzner S, Nauhaus I, Benucci A, Bonin V, Ringach DL, Carandini M. Local origin of field potentials in visual cortex. Neuron. 2009; 61:35–41. [PubMed: 19146811]
28. Mitzdorf U. Current source-density method and application in cat cerebral cortex: Investigation of evoked potentials and eeg phenomena. Physiol Rev. 1985; 65:37–100. [PubMed: 3880898]
29. Logothetis NK. The underpinnings of the bold functional magnetic resonance imaging signal. J Neurosci. 2003; 23:3963–71. [PubMed: 12764080]
30. Andersen RA, Musallam S, Pesaran B. Selecting the signals for a brain-machine interface. Curr Opin Neurobiol. 2004; 14:720–6. [PubMed: 15582374]
31. Pohlmeyer EA, Solla SA, Perreault EJ, Miller LE. Prediction of upper limb muscle activity from motor cortical discharge during reaching. J Neural Eng. 2007; 4:369–79. [PubMed: 18057504]
32. Mehring C, Nawrot MP, De Oliveira SC, Vaadia E, Schulze-Bonhage A, Aertsen A, Ball T. Comparing information about arm movement direction in single channels of local and epicortical field potentials from monkey and human motor cortex. Journal of physiology, Paris. 2004; 98:498–506.

33. Schalk G, Kubanek J, Miller KJ, Anderson NR, Leuthardt EC, Ojemann JG, Limbrick D, Moran D, Gerhardt LA, Wolpaw JR. Decoding two-dimensional movement trajectories using electrocorticographic signals in humans. J Neural Eng. 2007; 4:264–75. [PubMed: 17873429]
34. Hunter IW, Korenberg MJ. The identification of nonlinear biological systems: Wiener and hammerstein cascade models. Biol Cybern. 1986; 55:135–44. [PubMed: 3801534]
35. Westwick DT, Kearney RE. Identification of physiological systems: A robust method for non-parametric impulse response estimation. Med Biol Eng Comput. 1997; 35:83–90. [PubMed: 9136198]
36. Westwick DT, Pohlmeyer EA, Solla SA, Miller LE, Perreault EJ. Identification of multiple-input systems with highly coupled inputs: Application to emg prediction from multiple intracortical electrodes. Neural Comput. 2006; 18:329–55. [PubMed: 16378517]
37. Suminski AJ, Tkach DC, Fagg AH, Hatsopoulos NG. Incorporating feedback from multiple sensory modalities enhances brain-machine interface control. J Neurosci. 2010; 30:16777–87. [PubMed: 21159949]
38. Mackenzie, IS.; Kauppinen, T.; Silfverberg, M. Accuracy measures for evaluating computer pointing devices. Proceedings of the SIGCHI Conference on Human Factors in Computing Systems; Seattle, WA. 2001. p. 9-16.
39. Kim SP, Simeral JD, Hochberg LR, Donoghue JP, Black MJ. Neural control of computer cursor velocity by decoding motor cortical spiking activity in humans with tetraplegia. J Neural Eng. 2008; 5:455–76. [PubMed: 19015583]
40. Fitts PM. The information capacity of the human motor system in controlling the amplitude of movement. J Exp Psychol. 1954; 47:381–91. [PubMed: 13174710]
41. Mackenzie IS. A note on the information-theoretic basis of fitts' law. J Mot Behav. 1989; 21:323–30. [PubMed: 15136269]
42. Kennedy PR, Kirby MT, Moore MM, King B, Mallory A. Computer control using human intracortical local field potentials. IEEE Trans Neural Syst Rehabil Eng. 2004; 12:339–44. [PubMed: 15473196]
43. Hwang EJ, Andersen RA. Brain control of movement execution onset using local field potentials in posterior parietal cortex. J Neurosci. 2009; 29:14363–70. [PubMed: 19906983]
44. Leuthardt EC, Schalk G, Wolpaw JR, Ojemann JG, Moran DW. A brain-computer interface using electrocorticographic signals in humans. J Neural Eng. 2004; 1:63–71. [PubMed: 15876624]
45. Schalk G, Miller KJ, Anderson NR, Wilson JA, Smyth MD, Ojemann JG, Moran DW, Wolpaw JR, Leuthardt EC. Two-dimensional movement control using electrocorticographic signals in humans. J Neural Eng. 2008; 5:75–84. [PubMed: 18310813]
46. Felton EA, Wilson JA, Williams JC, Garell PC. Electrocorticographically controlled brain-computer interfaces using motor and sensory imagery in patients with temporary subdural electrode implants. Report of four cases J Neurosurg. 2007; 106:495–500.
47. Felton EA, Radwin RG, Wilson JA, Williams JC. Evaluation of a modified fitts law brain-computer interface target acquisition task in able and motor disabled individuals. J Neural Eng. 2009; 6:056002. [PubMed: 19700814]
48. Leuthardt EC, Miller KJ, Schalk G, Rao RP, Ojemann JG. Electrocorticography-based brain computer interface--the seattle experience. IEEE Trans Neural Syst Rehabil Eng. 2006; 14:194–8. [PubMed: 16792292]
49. Miller KJ, Schalk G, Fetz EE, Den Nijs M, Ojemann JG, Rao RP. Cortical activity during motor execution, motor imagery, and imagery-based online feedback. Proc Natl Acad Sci U S A. 2010; 107:4430–5. [PubMed: 20160084]
50. Gilja V, Nuyujukian P, Chestek CA, Cunningham JP, Yu BM, Fan JM, Churchland MM, Kaufman MT, Kao JC, Ryu SI, Shenoy KV. A high-performance neural prosthesis enabled by control algorithm design. Nat Neurosci. 2012:1752–8. [PubMed: 23160043]
51. Blakely T, Miller KJ, Zanos SP, Rao RP, Ojemann JG. Robust, long-term control of an electrocorticographic brain-computer interface with fixed parameters. Neurosurg Focus. 2009; 27:1–5.

52. Nuyujukian, P.; Kao, J.; Fan, J.; Stavisky, S.; Ryu, S.; Shenoy, K. A high-performance, robust brain-machine interface without retraining. The 9th annual Computation and Systems Neuroscience meeting; Salt Lake City, UT. 2012. p. 190III-65

53. Chao ZC, Nagasaka Y, Fujii N. Long-term asynchronous decoding of arm motion using electrocorticographic signals in monkeys. Front Neuroeng. 2010; 3:1–10. [PubMed: 20162033]

54. Perge, JA.; Homer, ML.; Malik, WQ.; Donoghue, JP.; Hochberg, LR. Decoding imagined arm movements from human motor cortex local field potentials. Program No. 583.09. 2012 Neuroscience Meeting Planner; New Orleans, LA: Society for Neuroscience; 2012. Online

55. Hochberg LR, Bacher D, Jarosiewicz B, Masse NY, Simeral JD, Vogel J, Haddadin S, Liu J, Cash SS, Van Der Smagt P, Donoghue JP. Reach and grasp by people with tetraplegia using a neurally controlled robotic arm. Nature. 2012; 485:372–5. [PubMed: 22596161]

56. Manohar A, Flint RD, Knudsen E, Moxon KA. Decoding hindlimb movement for a brain machine interface after a complete spinal transection. PLoS One. 2012; 7:e52173. [PubMed: 23300606]

57. Collinger JL, Wodlinger B, Downey JE, Wang W, Tyler-Kabara EC, Weber DJ, Mcmorland AJ, Velliste M, Boninger ML, Schwartz AB. High-performance neuroprosthetic control by an individual with tetraplegia. Lancet. 2013; 381:557–64. [PubMed: 23253623]

58. Markowitz DA, Wong YT, Gray CM, Pesaran B. Optimizing the decoding of movement goals from local field potentials in macaque cortex. J Neurosci. 2011; 31:18412–22. [PubMed: 22171043]

59. Taylor DM, Tillery SI, Schwartz AB. Direct cortical control of 3d neuroprosthetic devices. Science. 2002; 296:1829–32. [PubMed: 12052948]

60. Orsborn AL, Dangi S, Moorman HG, Carmena JM. Closed-loop decoder adaptation on intermediate time-scales facilitates rapid bmi performance improvements independent of decoder initialization conditions. IEEE Trans Neural Syst Rehabil Eng. 2012; 20:468–77. [PubMed: 22772374]

61. Danziger Z, Fishbach A, Mussa-Ivaldi FA. Learning algorithms for human-machine interfaces. IEEE Trans Biomed Eng. 2009; 56:1502–11. [PubMed: 19203886]

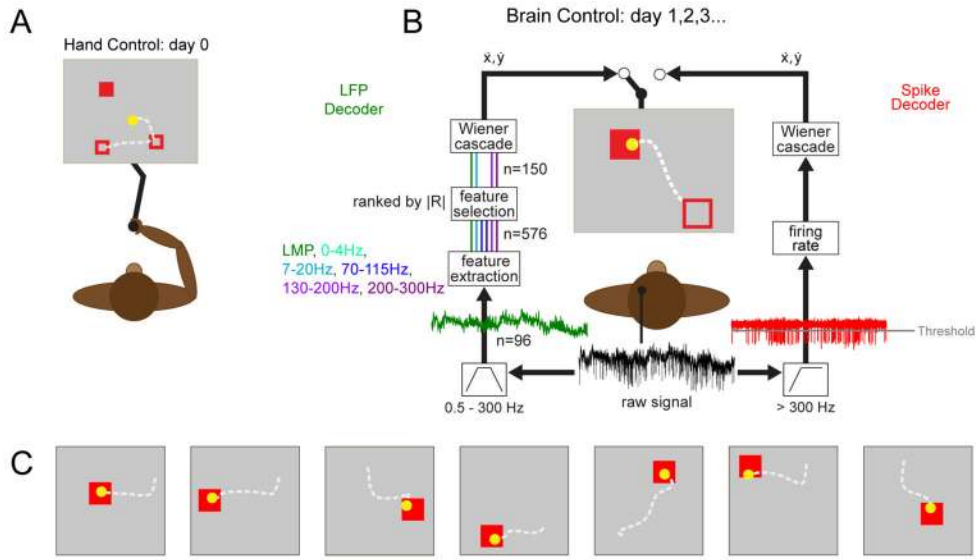

Figure 1.

Schematic of hand and brain control tasks. A, Random target pursuit task under hand control. Monkeys moved the cursor (yellow circle) to a series of targets (red squares). B, Monkeys performed brain control using either LFPs (left pathway) or MSPs (right pathway). Only one signal type at a time was used to decode velocity ($\dot{x}$,$\dot{y}$) for brain control. LMP, local motor potential (see Methods); R, Pearson's correlation coefficient. C, Example cursor trajectories under brain control.

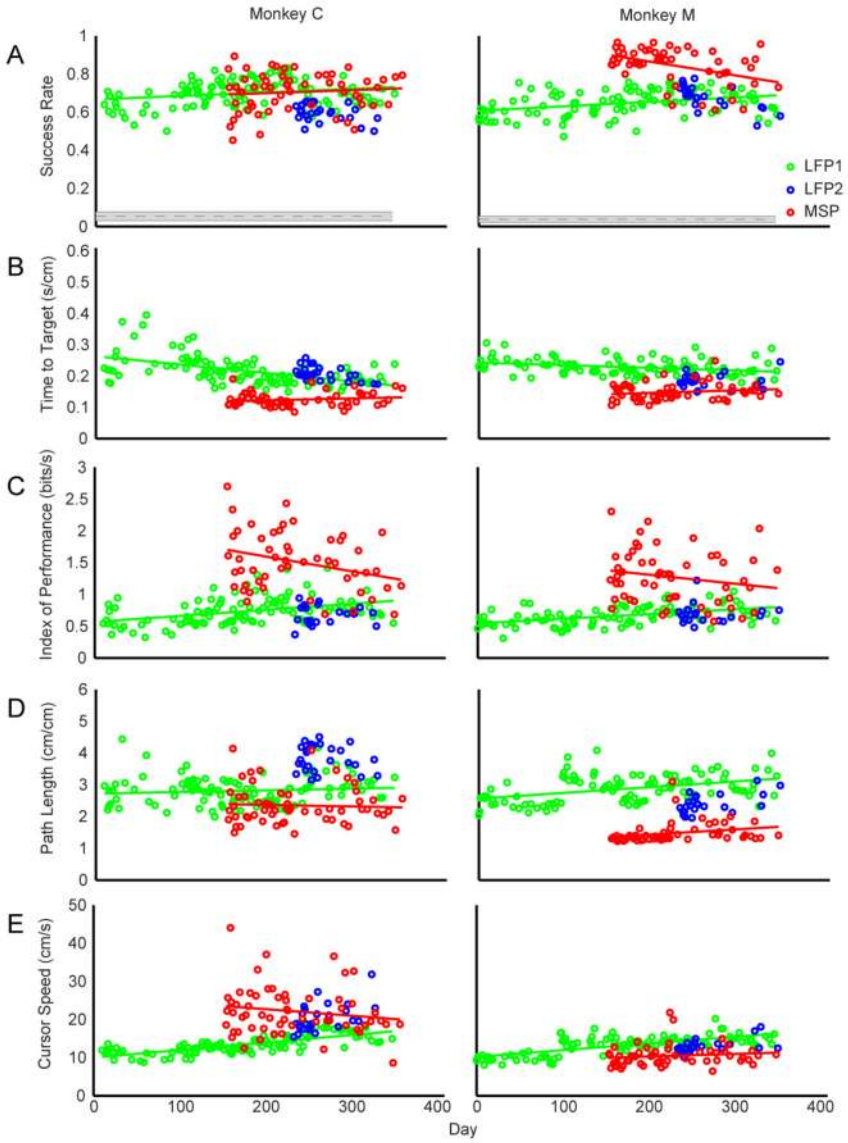

Figure 2.

Brain control performance trends. A, Success rate. Each circle is the ratio of successful trials to all trials for 1 epoch. The grey dashed lines and shaded areas show the mean and standard deviation of chance performance. B–E, Kinematic performance measures. Time to target, cursor speed, and path length were calculated for each trial; each circle represents the median across trials for 1 epoch. Solid lines through the LFP1 and MSP points are least-squares linear-fit lines.

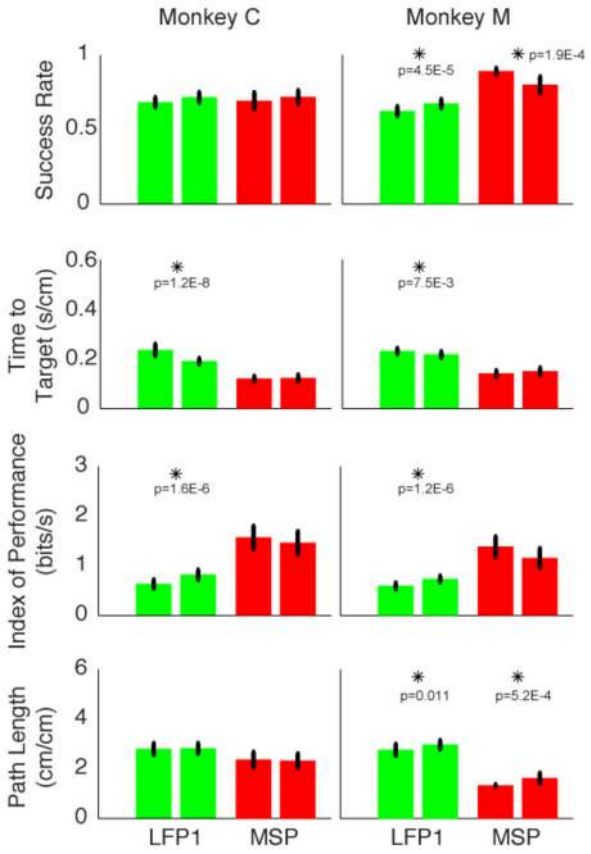

Figure 3.

Brain control performance in early (left bars) vs. late (right bars) epochs. Starred differences were significant at the $p<0.0125$ level (t-test, Bonferroni correction for multiple comparisons). Error bars represent standard deviation.

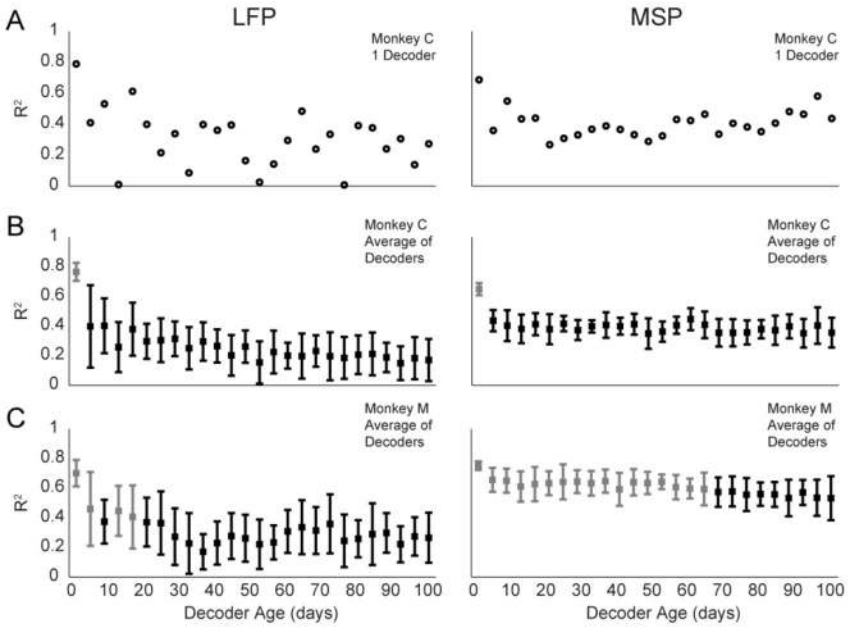

Figure 4.

Offline hand velocity decoding performance over time using static decoders. A) Decoding performance for a single LFP decoder (left panel) and a single MSP decoder (right panel) from monkey C. Note the day-to-day variability in performance after the first few days. B, C) When averaged across decoders, mean decoding performance declined significantly after day 0 in both (B) monkey C and in (C) monkey M using LFPs and MSPs. Error bars denote standard deviation. For monkey M's MSP-based decoding (C, right), the change in performance did not become significant until after day 64. In B and C, black error bars indicate significant differences from day 0 (1-way ANOVA for each panel, all main effects were significant ($p<0.001$), Tukey HSD post-hoc test, significance below $p=0.05$.

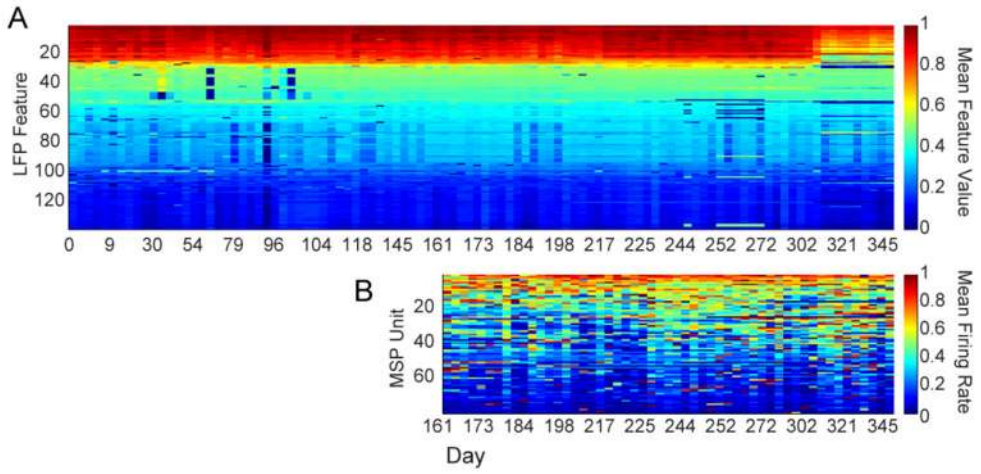

Figure 5.

Stability of LFP feature power and MSP firing rates for monkey M. A) Mean values in each epoch of the LFP features included in the fixed LFP1 decoder. B) Mean firing rates in each epoch of the units included in the fixed MSP decoder. We normalized feature values and firing rates to the maximum value for each feature or unit over all epochs, and sorted according to the values in the first epoch.

Table 1

Summary weekly statistics for BMI decoder use.

Epochs/Week, Min/Epoch, and Trials/Epoch are reported mean ± standard deviation.

Decoder	Time Span (days)	Total Epochs	Epochs/Week	Min/Epoch	Trials/Epoch
			Monkey C		
LFP1	340	110	2 ± 1	32 ± 15	268 ± 127
LFP2	96	26	2 ± 1	21 ± 10	131 ± 70
MSP	203	58	2 ± 1	22 ± 14	301 ± 205
			Monkey M		
LFP1	348	103	2 ± 1	27 ± 14	188 ± 96
LFP2	119	23	2 ± 2	27 ± 14	217 ± 134
MSP	195	54	2 ± 1	15 ± 6	220 ± 84

Table 2

Average performance over all epochs in each animal.
Mean ± standard deviation are reported for each decoder.

Decoder	Success Rate	Time to Target (s/cm)	Index of Performance (bits/s)	Path Length (cm/cm)	Cursor Speed (cm/s)
			Monkey C		
LFP1	0.70 ± 0.07	0.22 ± 0.05	0.73 ± 0.21	2.8 ± 0.4	13 ± 2
LFP2	0.60 ± 0.05	0.21 ± 0.02	0.68 ± 0.15	3.8 ± 0.4	20 ± 4
MSP	0.71 ± 0.10	0.12 ± 0.02	1.51 ± 0.46	2.3 ± 0.6	22 ± 6
			Monkey M		
LFP1	0.65 ± 0.07	0.23 ± 0.03	0.66 ± 0.15	2.9 ± 0.4	13 ± 2
LFP2	0.68 ± 0.06	0.19 ± 0.02	0.69 ± 0.15	2.4 ± 0.3	13 ± 2
MSP	0.85 ± 0.09	0.15 ± 0.03	1.27 ± 0.42	1.5 ± 0.3	10 ± 3

Table 3

Pearson's correlation coefficient (R) between performance measures and time.

Significant values of R ($p<0.01$; Bonferroni-corrected for multiple comparisons) that reflect worsening performance are grey, and those reflecting improving performance are boldface. Non-significant correlations indicate the measure was stable over time. No interpretation was made as to whether increased cursor speed represented an improvement or a decline in performance.

Decoder	Success Rate	Time to Target (s/cm)	Index of Performance (bits/s)	Path Length (cm/cm)	Cursor Speed (cm/s)
			Monkey C		
LFP1	R=0.23 p=0.02	**R=–0.52** **p=7E-9**	**R=0.39** **p=2E-5**	R=0.1 p=0.28	R=0.72 p=4E-19
LFP2	R=–0.41 p=0.04	**R=–0.57** **p=0.002**	R=–0.03 p=0.89	R=–0.14 p=0.48	R=0.55 p=0.003
MSP	R=0.09 p=0.49	R=0.16 p=0.23	R=–0.30 p=0.03	R=–0.05 p=0.70	R=–0.16 p=0.22
			Monkey M		
LFP1	**R=0.35** **p=4E-4**	**R=–0.31** **p=0.001**	**R=0.46** **p=2E-6**	R=0.41 p=2E-5	R=0.7 p=4E-16
LFP2	R=–0.71 p=2E-4	R=0.12 p=0.60	R=0.03 p=0.90	R=0.58 p=3E-3	R=0.53 p=9E-3
MSP	R=–0.43 p=0.001	R=0.17 p=0.23	R=–0.19 p=0.17	R=0.27 p=0.05	R=0.13 p=0.34